RSC Advances




ROYAL SOCIETY OF CHEMISTRY

www.rsc.org/advances

Silver nanowires were successfully synthesized by a polyol reduction method in a continuous-flow reactor with the yield of 2 g/h.

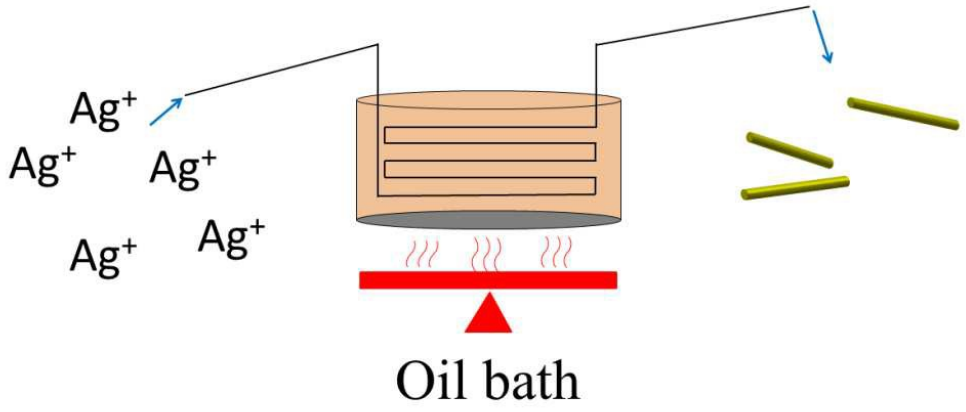

# Salt-mediated polyol synthesis of silver nanowires in a continuous-flow tubular reactor

Kan-Sen Chou[1], Chung-Yen Hsu[1], and Bo-Tau Liu[2,*]

[1]Department of Chemical Engineering
National Tsing Hua University
Hsinchu 30013, Taiwan

[2]Department of Chemical and Materials Engineering
National Yunlin University of Science and Technology
Yunlin 64002, Taiwan



*Corresponding author: Department of Chemical and Materials Engineering, National, Yunlin University of Science and Technology, 123 Univ. Rd., Sec. 3, Douliou, Yunlin 64002, Taiwan, ROC. Tel.: 886-5-534-2601. Fax: 886-5-531-2071.
E-mail address: liubo@yuntech.edu.tw (B.-T. Liu).

**ABSTRACT**

This study is the first time to present the synthesis of silver nanowires by a polyol reduction method in a continuous-flow reactor. The effects of process parameters on the conversion, selectivity, and morphology of silver nanowires are analyzed. Experimental results reveal that sufficient space time, low reaction temperature, and moderate molar ratio of polyvinylpyrrolidone (PVP) to silver ions can result in high conversion (97.16%) and selectivity (near 100%). Normally, in our system the yield can reach to 2 g/h and the resulting AgNWs have the average length of 22 $\mu$m and diameter of 90 nm. It is found that the length of AgNWs can be adjusted by varying the initial concentration of silver ions and the PVP amount, and the diameter can be reduced with increasing the concentration of potassium chloride. Unlike the batch system, it doesn't hinder the growth of silver nanowires that all of the reactants are added simultaneously into the reactor for the continuous-flow system, resulting from the formation of pre-seeds and the rapid rise of temperature in the tubular reactor.

Key words: Silver nanowire; Continuous-flow; Conversion; Selectivity

## 1. **Introduction**

1-D nano-materials have received increasing attention due to their extraordinary optoelectronic, magnetic, and catalytic properties.[1-3] Especially, silver nanowires (AgNWs) display excellent conductivity through electron conduction on the axial direction and very high ratio of DC conductivity to optical conductivity, which have been widely investigated in the applications of transparent conductive films, catalysis, conductive nanocomposites, sterilization, and surface Raman spectroscopy enhancement.[4-8] Numerous methods have been reported in the literature for the synthesis of AgNWs, such as template,[9, 10] hydrothermal,[11, 12] low-temperature growth,[13] thermal-induced formation,[14] microwave assistance,[15, 16] photo-reduction,[17] and polyol method.[18] Among those, the salt-mediated polyol method extended by Xia's group [19-23] is the most promising and popular because the method doesn't need expansive equipments and has higher yield than others.

Although the preparation process for the polyol method is simple, the quality of the as-prepared AgNWs is very sensitive to the process parameters; the aspect ratio and the yield of AgNWs depend strongly on kinds of inorganic salts,[24, 25] ratio of salt to silver nitrate,[26] molecular weight of polyvinylpyrrolidone (PVP),[27] ratio of PVP to silver nitrate,[25] reaction temperature,[26, 28] reaction time,[5] atmosphere,[29, 30] and reagent-addition procedure.[23, 28] Therefore, a similar preparation process with a little

variation usually leads to significantly different results for AgNW production.[28, 31] Many efforts have been exerted to control quality of AgNWs to increase their applicability. Up to now, all of the studies for the synthesis of AgNWs are still limited to batch systems. Each batch produces only a small AgNW amount. Even for the high-concentration synthesis, the yield is only 0.5-1 g each time,[32-34] restricted to meet the growing AgNW requirements.

To the best of our knowledge, no continuous-flow systems have been investigated for AgNW production; the relevant studies on the continuous-flow production are few and only for silver nanoparticles.[35] Due to the versatile characterization, it becomes more difficult to synthesize AgNWs in a continuous-flow reactor. In this study, we investigated the synthesis of AgNWs by a one-step synthesis method in a continuous-flow reactor. Effects of reaction time, PVP amount and reaction temperature on the quality of AgNWs were analyzed. Finally, the high conversion and the yield of 2 g/h have been carried out in our system.

## 2. Experimental

### 2.1 Materials

Silver nitrate ($AgNO_3$, Kojima), PVP (Sigma–Aldrich), ethylene glycol (EG, Scharlau), and potassium chloride (KCl, Pure Chemical Industries) were used as

received. Reagent-grade solvents and deionized water (DI water, >18 MΩ·cm) were used throughout the experiments.

2.2 Preparation of AgNWs in a continuous-flow tubular reactor

AgNWs were synthesized using a one-step polyol reduction method in a continuous tubular reactor. The reaction system was set as shown in Fig.1; a tubular glass coil with inner diameter of 6 mm and outer diameter of 8 mm was placed into a silicone-oil bath. The S0 solution (PVP in EG) and the silicone-oil bah was pre-heated to the reaction temperature (150, 160, and 170 ℃), whereas the S1 solution ($AgNO_3$ and KCl in EG) remained at room temperature. Before starting up the reaction, all of the pipes and the tubular reactor were rinsed with EG. The S0 and S1 solutions then flowed into the tubular reactor at a certain constant rate (normally, 6.46-11.06 ml/min) using a peristaltic pump. The AgNW synthesis was investigated with respect to various space times, which were regulated by virtue of the change of inlet flow rate. Unless otherwise indicated, the molecular weight of PVP used in S0 is 360 k, the concentration of $AgNO_3$ in S1 solution is 0.0588 M, and the molar ratio of KCl to $AgNO_3$ is 0.01. The effluents were further evaluated and analyzed to judge the quality of the production. After the end of an experiment, the loop was cleaned with a dilute nitric-acid solution to avoid that the residues of silver salts or bulk silver affected next experiment, and further rinsed with water and ethanol.

2.3 Characterization

The morphology of AgNWs was examined using an optical microscope (OM, BX51M, Olympus) and a cold-field-emission scanning electron microscope (SEM, SU8010, Hitachi). The calculation of distribution and average for the length and diameter of AgNWs is based on 100 nanowires observed from the SEM images. The conversion of silver products (including AgNWs and Ag nanoparticles) was calculated from the following equation

$$\text{Conversion} = \frac{[Ag^+]_i - [Ag^+]_o}{[Ag^+]_i} \times 100\% , \quad (1)$$

where $[Ag^+]_i$ and $[Ag^+]_o$ are the inlet and outlet concentrations of silver ions, respectively. The concentration of silver ions was determined using an ion selective electrode (EW-27504-28, Cole Parmer).

## 3. Results and discussion

As aforementioned in Introduction that the quality of AgNW production depends on many reaction parameters, including reaction temperature, space time (reaction time), molecular weight of PVP, and concentration of reactants ($AgNO_3$, KCl, and PVP). In order to simplify the analysis for the AgNW-production system, we

optimized the conversion of metallic silver and the selectivity of AgNWs first, and then controlled the aspect ratio of AgNWs with regard to these parameters.

3.1 Conversion and selectivity in the continuous-flow system

According to the experience of AgNW synthesis in the batch system,[27] we started up the AgNW synthesis with the reaction conditions: reaction temperature =160 ℃, the weight ratio of PVP/$AgNO_3$ =1.66. The reaction parameters were then adjusted as shown in Table 1 to optimize the AgNW-synthesis process. Because the length of the flowing conduit of the coil reactor is constant, the space time (reaction time) was changed by varying the flow rate. As shown in Table 1, the conversion increases with the increase of the space time and reaches to 97.13% when the space time increases to 13.5 min. Many silver nanoparticles form in the effluent flow for short space times (Figs. 2a-b), whereas the nanoparticles disappear when the space time is long enough (Fig. 2c), indicating that the nanoparticles form at the early stage of the reaction and then transform gradually into nanowires. The result is consistent with the observation in the batch system.[32, 36] The conversion also depends on the weight ratio of PVP/$AgNO_3$. When the ratio is low, the conversion reduces (Table 1) and nanoparticles appear in the final product (namely, the AgNW selectivity reduces) (Fig. 2d), whereas the conversion increases slightly but the variation of the AgNW selectivity is unobservable when the ratio increases (Fig. 2e), revealing that PVP not

only promotes the formation of AgNWs but is also helpful for the reduction of silver ions.[37] When the reaction temperature is raised to 170 ℃, the conversion increases slightly but some short nanowires, nanorods, and nanoparticles form in the final products as well (Fig. 2f). However, when the reaction temperature is reduced to 150 ℃, the AgNWs become more uniform (Fig. 2g) and the selectivity is near 100%. The resulting AgNWs have the average length of 22 $\mu$m (Fig. 3) and diameter of 90 nm (Fig. 2g), and the corresponding AgNW yield reaches to 2 g/h.

3.2 Control on length of AgNWs

Referring to Fig. 3, the length of AgNWs depends on the initial concentration of silver ions; the length of AgNWs decrease with decreasing the initial concentration of silver ions. This may result from the fact that the growth of AgNWs relies on the supply of the silver ions. However, according to the mass balance, the decrease of the initial concentration will lead to decreasing the AgNW yield. We found the AgNW length also depends on the amount of PVP. With increasing the PVP amount in use, the length of AgNWs decreases and some silver nanoparticles appear, as shown in Fig. 4. This may be attributed to excess PVP can adsorbing on the {111} facets of AgNWs and thus passivating the growth of nanowires and forming nanoparticles. In addition, the molecular weight of PVP also influences the AgNW length. When the molecular weight of PVP is changed from 360 k to 40 k, the AgNW length decreases remarkably

(Fig. 5a); when the very-low-molecular-weight PVP (3.5 k) is used, many particle aggregates appear (Fig. 5b). The chain length of PVP is proportional to its molecular weight, so the low-molecular-weight PVP with possesses a shorter chain. The shorter chain may have worse anisotropic characteristics [38] and can't form a soft template for the connection of nanorods or nanoparticles to form the AgNWs.[36]

3.3 Control on diameter of AgNWs

Fig. 6a shows the diameter of the AgNWs synthesized with various molar ratio of $KCl/AgNO_3$; the diameter decreases gradually with increasing the ratio (Fig. S1). Fortunately, the length of AgNWs is almost independent of the ratio of $KCl/AgNO_3$ (Fig. 6b). Chloride ions play a key role on the formation of AgNWs. Some studies reported that the AgCl precipitates induced by the chloride ions could slow down the reaction rate by virtue of the slow release of silver ions form the precipitates and consequently made anisotropic growth of AgNWs favorable.[39] In our experiments, the silver ions and chloride ions were added simultaneously into the continuous-flow reactor and the amount of silver ions is much larger than that of chloride ions. As a result, the chloride ions serve as a reaction-rate controller is less possible. Besides, chloride ions are supposed to have two functions in the synthesis process: one is form AgCl precipitates in the beginning of the reaction serving as seeds for five-twinned particles, and the other is to selectively adsorb on {100} facets serving as a inhibitor

to retard crystal growth.[26, 40] We speculate that more chloride ions results in the formation of more AgCl precipitates and thereby form more multi-twinned seeds; the more AgCl precipitates also restrict more the growth of the {100} facets, as observed in the batch system. The results lead to smaller diameter but unchanged length.

3.4 Comparison between continuous-flowing reaction and batch reaction

Although the sampling on different positions of the reactor tube is unavailable in our present system, the crystalline structure of the Ag particles synthesized at short space time and the as-prepared AgNWs was found to be the same as that synthesized from the batch reactor, which implies both may have the same nucleation and growth mechanisms. However, for batch system, the $AgNO_3$ is usually added slowly into the PVP solution; too fast addition will hinder the formation of AgNWs.[23] In our continuous-flow system, all of the reactants were added simultaneously into the reactor, but the AgNWs still form well. To further realize the cause, we further analyzed the variation of the temperature insider the tubular reactor. In all our experiments, the flow inside the tubular reactor is laminar. For example, the Reynolds number is 9.8 as the space time is 30 min. The heat transfer coefficient *h* for the laminar flow inside the helical coil reactor can be calculated from the Manlapaz-Churchill correlation[35, 41]:

$$h = \frac{k}{d} \times \mathrm{Nu} = \left[ \left( 3.657 + \frac{4.343}{\left( 1 + \frac{957}{\mathrm{Pr} \times \mathrm{He}^2} \right)^2} \right)^3 + 1.158 \times \left( \frac{\mathrm{He}}{1 + \frac{0.477}{\mathrm{Pr}}} \right)^{3/2} \right]^{1/3} \quad (2)$$

In the expression, $k$ and $d$ are the thermal conductivity of the fluid and the inert diameter of the tube, respectively; Nu, Pr, and He are the Nusselt number, the Prandtl number, and the helical number, respectively. Therefore, the temperature of the fluid along the tubular reactor can be estimated as

$$T = \frac{T_i + \frac{\pi \times d \times h \times \tau \times t}{m \times C_p} T_b}{1 + \frac{\pi \times d \times h \times \tau \times t}{m \times C_p}} \quad (3)$$

where $T_i$ and $T_b$ are the entering temperature of the fluid and the temperature of the oil bath, respectively; $\tau$, $t$, $m$, and $C_p$ are the space time, the residence time, the mass flow rate, and the specific heat of the fluid. Fig. 7 shows the variation of the temperature inside the reactor with the residence time. For the tubular reactor, the temperature of the fluid rises rapidly and reaches 140 ℃ at t ≈ 2.3 min. In order to know the difference between the variation of temperature for continuous-flow and that for batch systems, 12 ml of S1 solution (room temperature) was added immediately into 12 ml of S0 solution (150 ℃) in a batch reactor under 100-rpm stirring, where the theoretic output of the AgNW production is 0.089 g, and the variation on the temperature of the solution was recorded in Fig. 7. The rise of the temperature for the batch reaction with

the residence time is slower than that for the continuous-flow reaction and the time requires near 5.5 min for the temperature reaching to 140 ℃. The as-prepared AgNWs for the batch reaction system is short (< 3 μm, mostly, shown in Fig. S2a). If the reaction solution for the batch system is reduced by half, which rise of the temperature of the solution is very similar to that of the continuous-flow system (Fig. 7), the as-prepared AgNWs become longer (Fig. S2b). Since the reduction rate of silver ions at a lower reaction temperature is much slower, the long temperature-rising period may result in a long nucleation period, short AgNWs, and formation of various silver structures.[26, 28] Moreover, we also found that it was necessary for the continuous production of AgNWs that $AgNO_3$ and KCl had to be mixed to form AgCl precipitates serving as seeds for the five-twinned crystals before they were delivered into the reaction tube; otherwise, the yield of AgNWs reduces and the silver particles increase. We simulated the condition in the batch reactor with low stirring rate (100 rpm). If $AgNO_3$ and KCl wasn't pre-mixed, many silver particles form (Fig. S2c) and the yield of AgNWs decreases (Fig. S3). We infer that the mixing is not well in the tubular reactor at low flow rate, so the pre-mixing is important to the formation of silver crystals, resulting in nanowire growth.

## 4. Conclusion

We have successfully synthesized the AgNWs by the polyol reduction method in a continuous-flow reactor with the yield of 2 g/h, which is much larger than that of batch systems. The conversion and selectivity can reach to 97.16% and near 100%, respectively. The resulting AgNWs have the average length of 22 $\mu$m and diameter of 90 nm. The length of AgNWs can be adjusted by varying the initial $AgNO_3$ concentration and the PVP amount, and the diameter is found to decrease with the ratio of $KCl/AgNO_3$. The effects of process parameters on the AgNW synthesis for the continuous-flow system are similar to those for the batch system as reported elsewhere. Compared with batch systems, the most difference for the continuous-flow systems is to add all of the reactants at the same time. However, the process is not found to hinder the growth of AgNWs in our experiments. The result may be explained from the fact that the temperature of the solution rises rapidly in the tubular reactor and the seeds are pre-formed.

**Acknowledgments**

This study was supported financially by the Ministry of Science and Technology of the Republic of China.

## References


1. C. Vakifahmetoglu, *Adv. Appl. Ceram.*, 2011, **110**, 188-204.
2. M. de la Mata, X. Zhou, F. Furtmayr, J. Teubert, S. Gradecak, M. Eickhoff, A. F. I. Morral and J. Arbiol, *J. Mater. Chem. C*, 2013, **1**, 4300-4312.
3. K. Balasubramanian, *Biosensors & Bioelectronics*, 2010, **26**, 1195-1204.
4. S. Sorel, P. E. Lyons, S. De, J. C. Dickerson and J. N. Coleman, *Nanotechnology*, 2012, **23**, 185201.
5. S. M. Bergin, Y. H. Chen, A. R. Rathmell, P. Charbonneau, Z. Y. Li and B. J. Wiley, *Nanoscale*, 2012, **4**, 1996-2004.
6. M. Wen, B. L. Sun, B. Zhou, Q. S. Wu and J. Peng, *J. Mater. Chem.*, 2012, **22**, 11988-11993.
7. B.-T. Liu and H.-L. Kuo, *Carbon*, 2013, **63**, 390-396.
8. A. Tao, F. Kim, C. Hess, J. Goldberger, R. R. He, Y. G. Sun, Y. N. Xia and P. D. Yang, *Nano Lett.*, 2003, **3**, 1229-1233.
9. T. A. Crowley, K. J. Ziegler, D. M. Lyons, D. Erts, H. Olin, M. A. Morris and J. D. Holmes, *Chem. Mater.*, 2003, **15**, 3518-3522.
10. E. Braun, Y. Eichen, U. Sivan and G. Ben-Yoseph, *Nature*, 1998, **391**, 775-778.
11. T. Tetsumoto, Y. Gotoh and T. Ishiwatari, *J. Colloid Interface Sci.*, 2011, **362**, 267-273.

12. J. Xu, J. Hu, C. J. Peng, H. L. Liu and Y. Hu, *J. Colloid Interface Sci.*, 2006, **298**, 689-693.

13. S. H. Kim, B. S. Choi, K. Kang, Y. S. Choi and S. I. Yang, *J. Alloys Compd.*, 2007, **433**, 261-264.

14. T. K. Chen, W. T. Chen, M. C. Yang and M. S. Wong, *J. Vac. Sci. Technol., B*, 2005, **23**, 2261-2265.

15. M. Tsuji, Y. Nishizawa, K. Matsumoto, N. Miyamae, T. Tsuji and X. Zhang, *Colloids Surf. A*, 2007, **293**, 185-194.

16. L. F. Gou, M. Chipara and J. M. Zaleski, *Chem. Mater.*, 2007, **19**, 1755-1760.

17. Z. Xie, Z. Y. Wang, Y. X. Ke, Z. G. Zha and C. Jiang, *Chem. Lett.*, 2003, **32**, 686-687.

18. R. Zhu, C. H. Chung, K. C. Cha, W. B. Yang, Y. B. Zheng, H. P. Zhou, T. B. Song, C. C. Chen, P. S. Weiss, G. Li and Y. Yang, *ACS Nano*, 2011, **5**, 9877-9882.

19. Y. G. Sun, B. Gates, B. Mayers and Y. N. Xia, *Nano Lett.*, 2002, **2**, 165-168.

20. Y. G. Sun and Y. N. Xia, *Adv. Mater.*, 2002, **14**, 833-837.

21. K. E. Korte, S. E. Skrabalak and Y. N. Xia, *J. Mater. Chem.*, 2008, **18**, 437-441.

22. Y. G. Sun, B. Mayers, T. Herricks and Y. N. Xia, *Nano Lett.*, 2003, **3**, 955-960.

23. Y. G. Sun, Y. D. Yin, B. T. Mayers, T. Herricks and Y. N. Xia, *Chem. Mater.*, 2002, **14**, 4736-4745.

24. C. Chen, L. Wang, G. H. Jiang, J. F. Zhou, X. Chen, H. J. Yu and Q. Yang, *Nanotechnology*, 2006, **17**, 3933-3938.

25. D. P. Chen, X. L. Qiao, X. L. Qiu, J. G. Chen and R. Z. Jiang, *J. Mater. Sci. - Mater. Electron.*, 2011, **22**, 6-13.

26. X. L. Tang, M. Tsuji, M. Nishio and P. Jiang, *Bull. Chem. Soc. Jpn.*, 2009, **82**, 1304-1312.

27. Y. C. Lu and K. S. Chou, *Nanotechnology*, 2010, **21**, 215707.

28. S. Coskun, B. Aksoy and H. E. Unalan, *Cryst. Growth Des.*, 2011, **11**, 4963-4969.

29. X. L. Tang, M. Tsuji, P. Jiang, M. Nishio, S. M. Jang and S. H. Yoon, *Colloids Surf. A*, 2009, **338**, 33-39.

30. B. Wiley, T. Herricks, Y. G. Sun and Y. N. Xia, *Nano Lett.*, 2004, **4**, 1733-1739.

31. Y. C. Lu, K. S. Chou and M. Nogami, *Mater. Chem. Phys.*, 2009, **116**, 1-5.

32. M. J. Hu, J. F. Gao, Y. C. Dong, S. L. Yang and R. K. Y. Li, *RSC Adv.*, 2012, **2**, 2055-2060.

33. B.-T. Liu, S.-X. Huang, M.-F. Lai and Z.-H. Wei, *RSC Adv.*, 2015, **5**, 1684-1689.

34. B.-T. Liu and S.-X. Huang, *RSC Adv.*, 2014, **4**, 59226-59232.

35. X. Z. Lin, A. D. Terepka and H. Yang, *Nano Lett.*, 2004, **4**, 2227-2232.

36. C. L. Kuo and K. C. Hwang, *Langmuir*, 2012, **28**, 3722-3729.

37. Z. T. Zhang, B. Zhao and L. M. Hu, *J. Solid State Chem.*, 1996, **121**, 105-110.

38. M. Tsuji, Y. Nishizawa, K. Matsumoto, M. Kubokawa, N. Miyamae and T. Tsuji, *Mater. Lett.*, 2006, **60**, 834-838.

39. Z. H. Wang, J. W. Liu, X. Y. Chen, J. X. Wan and Y. T. Qian, *Chem. Eur. J.*, 2005, **11**, 160-163.

40. S. H. Im, Y. T. Lee, B. Wiley and Y. N. Xia, *Angew. Chem. Int. Ed.*, 2005, **44**, 2154-2157.

41. R. L. Manlapaz and S. W. Churchill, *Chem. Eng. Commun.*, 1981, **9**, 185-200.

**List of figures**

Fig. 1. Schematic representation of the continuous-flow system.

Fig. 2. OM images of the AgNW products synthesized under various reaction conditions: (a) P1, (b) P2, (c) P3, (d) P4, (e) P5, (f) P6, and (g) P7 listed in Table 1. (h) SEM image of AgNWs synthesized at the P3 condition.

Fig. 3. Variation of the length of AgNWs versus the initial concentration of $AgNO_3$. Reaction conditions: space time = 30 min, reaction temperature = 150 ℃, $PVP/AgNO_3$ = 1.66.

Fig. 4. OM images of the AgNW products synthesized at various weight ratios of $PVP/AgNO_3$: (a) 2.5, (b) 2.91. Reaction conditions: space time = 30 min, reaction temperature = 150 ℃.

Fig. 5. OM images of the AgNW products synthesized at various molecular weights of PVP: (a) 40 k, (b) 3.5 k. Reaction conditions: space time = 30 min, reaction temperature = 150 ℃, $PVP/AgNO_3$ = 1.66.

Fig.6 Variation of (a) the diameter versus the molar ratio of $KCl/AgNO_3$ and (b) the corresponding length. Reaction conditions: space time = 30 min, reaction temperature = 150 ℃, $PVP/AgNO_3$ = 1.66.

Fig. 7. Variation of the temperature inside the reactor verse the residence time. Solid line: the result calculated from eq. (1) for the present continuous-flow tubular

reactor. Parameters used: $\tau$ = 30 min, $k$ = 0.2579 W/m·K , $Cp$ = 0.58 Btu/ℓb·$^{o}$F , viscosity = 5.2 cp, and density = 1.115 g/cm$^{3}$; ■: the experimental data for adding 12 ml of S1 solution (room temperature) into 12 ml of S0 solution (150 ℃) in a batch reactor under 100-rpm stirring; ●: the same as the case of ■, except that both S0 and S1 are 6 ml.

Table 1. Effects of process parameters on conversion.

| Process parameters | | | | Conversion, % |
|---|---|---|---|---|
| Code | Space time, min | Reaction temperature, ℃ | PVP/$AgNO_3$, mol./mol. | |
| P1 | 8 | 160 | 1.66 | 78.25 |
| P2 | 10 | 160 | 1.66 | 88.32 |
| P3 | 13.5 | 160 | 1.66 | 97.13 |
| P4 | 13.5 | 160 | 0.583 | 87.52 |
| P5 | 13.5 | 160 | 2.33 | 98.72 |
| P6 | 13.5 | 170 | 1.66 | 98.20 |
| P7 | 30 | 150 | 1.66 | 97.16 |

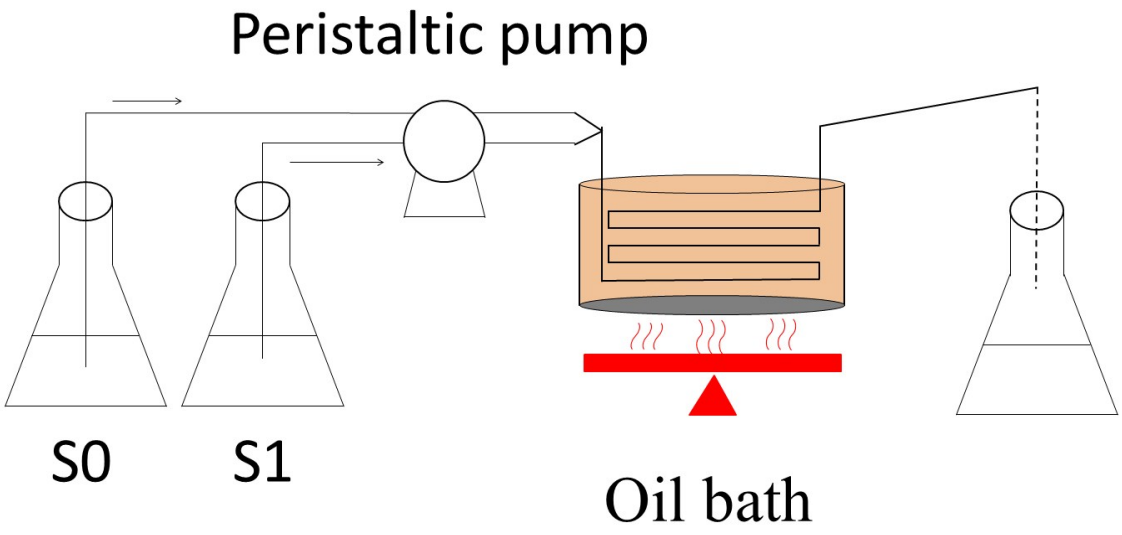


Fig. 1. Schematic representation of the continuous-flow system.

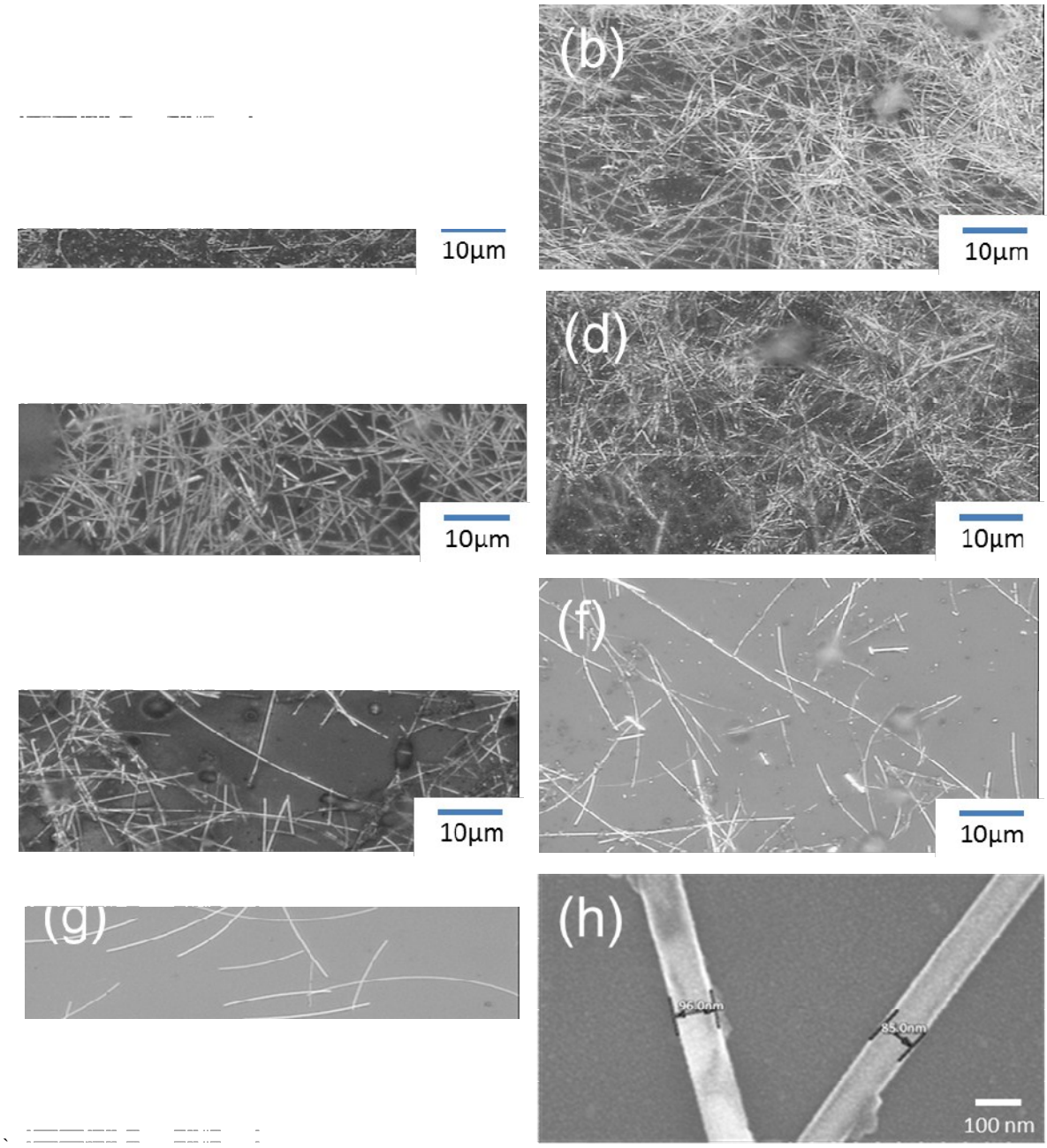


Fig. 2. OM images of the AgNW products synthesized under various reaction conditions: (a) P1, (b) P2, (c) P3, (d) P4, (e) P5, (f) P6, and (g) P7 listed in Table 1. (h) SEM image of AgNWs synthesized at the P3 condition.

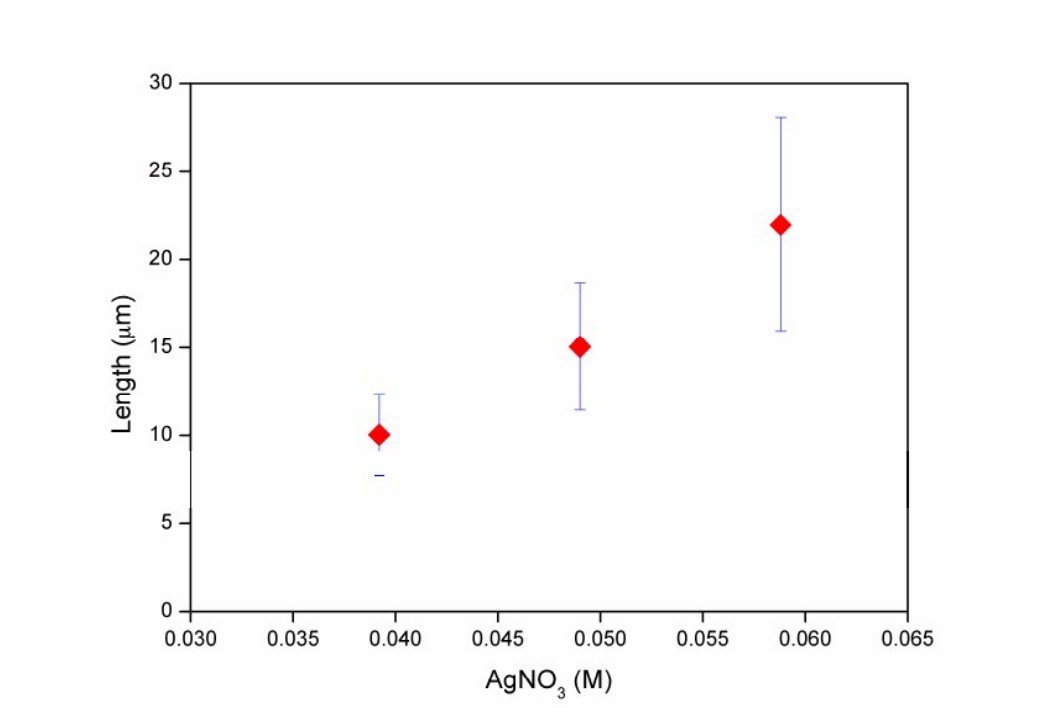


Fig. 3. Variation of the length of AgNWs versus the initial concentration of $AgNO_3$. Reaction conditions: space time = 30 min, reaction temperature = 150 ℃, PVP/$AgNO_3$ = 1.66.

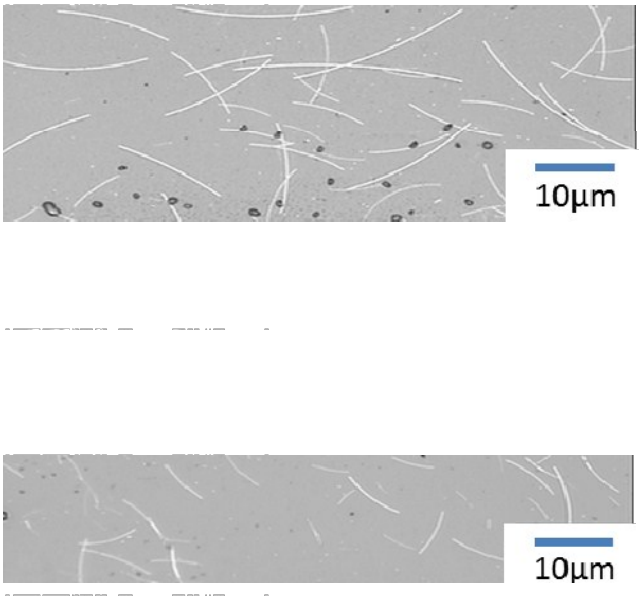


Fig. 4. OM images of the AgNW products synthesized at various weight ratios of PVP/$AgNO_3$: (a) 2.5, (b) 2.91. Reaction conditions: space time = 30 min, reaction temperature = 150 ℃.

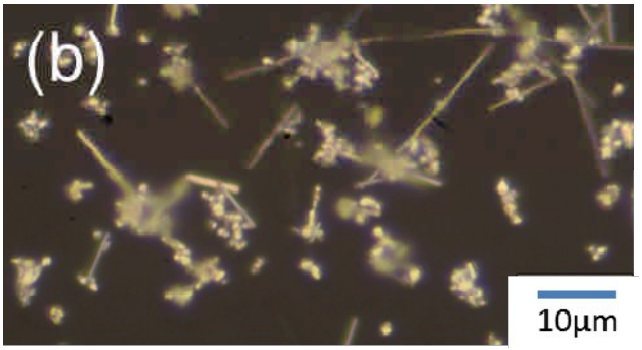


Fig. 5. OM images of the AgNW products synthesized at various molecular weights of PVP: (a) 40 k, (b) 3.5 k. Reaction conditions: space time = 30 min, reaction temperature = 150 ℃, PVP/$AgNO_3$ = 1.66.

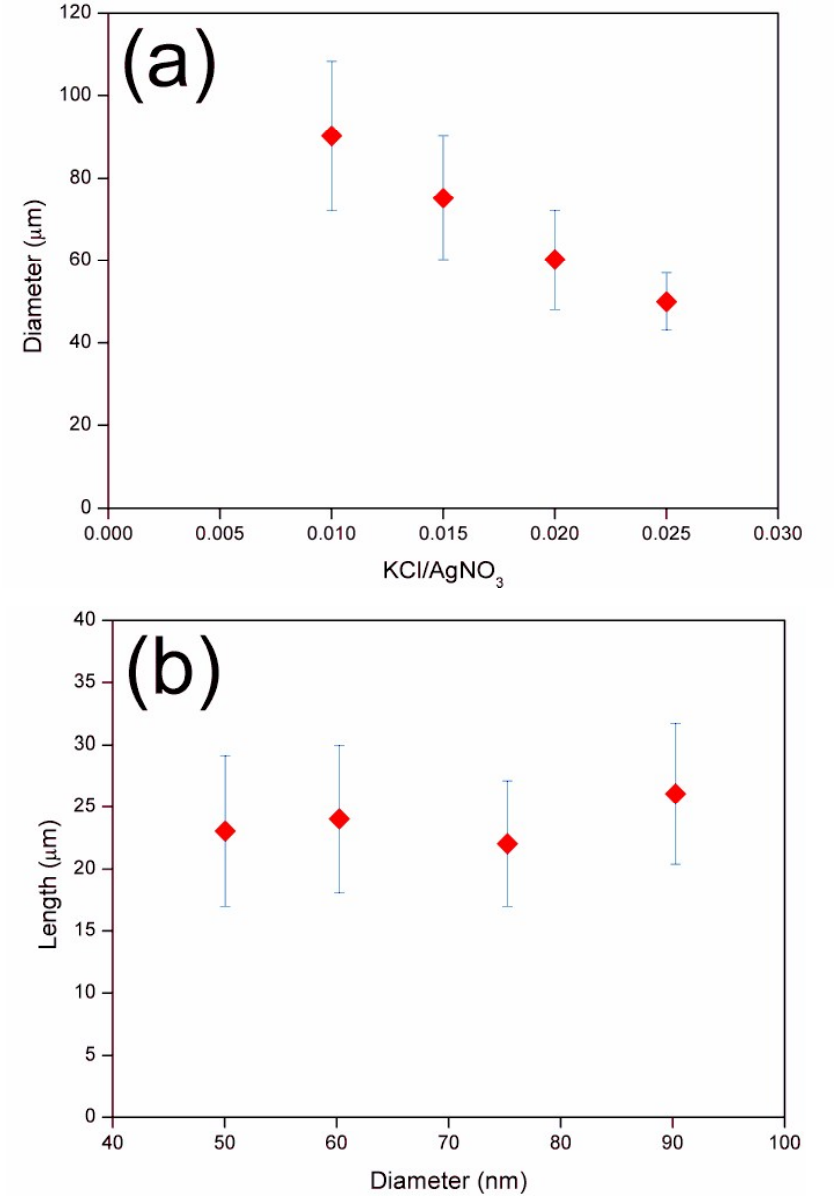


Fig. 6. Variation of (a) the diameter versus the molar ratio of $KCl/AgNO_3$ and (b) the corresponding length. Reaction conditions: space time = 30 min, reaction temperature = 150 ℃, $PVP/AgNO_3$ = 1.66.

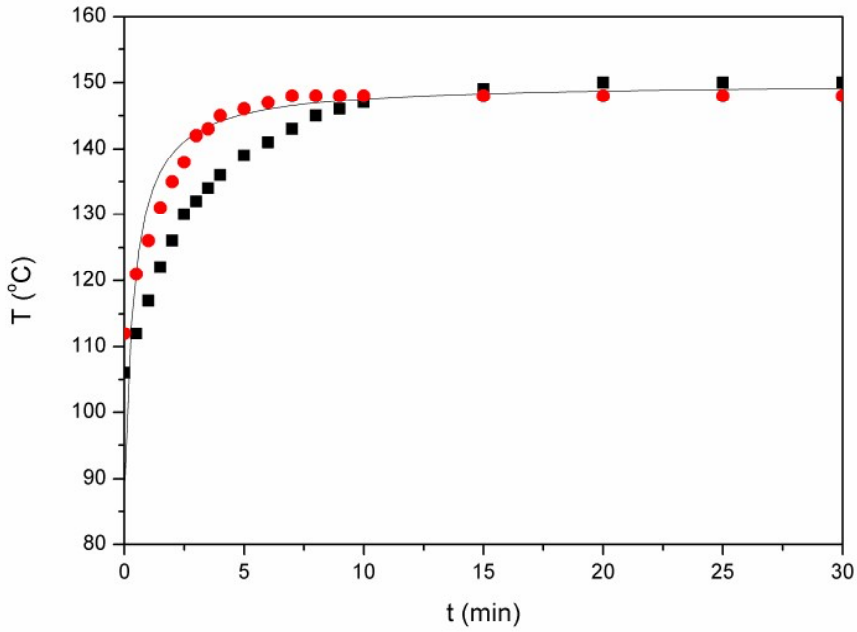


Fig. 7. Variation of the temperature inside the reactor verse the residence time. Solid line: the result calculated from eq. (1) for the present continuous-flow tubular reactor. Parameters used: $\tau$ = 30 min, $k$ = 0.2579 W/m·K, $Cp$ = 0.58 Btu/ℓb·°F, viscosity = 5.2 cp, and density = 1.115 g/cm$^3$; ■: the experimental data for adding 12 ml of S1 solution (room temperature) into 12 ml of S0 solution (150 ℃) in a batch reactor under 100-rpm stirring; ●: the same as the case of ■, except that both S0 and S1 are 6 ml.